Eur. Phys. J. Special Topics **165**, 5–14 (2008)

DOI: 10.1140/epjst/e2008-00844-2

THE EUROPEAN PHYSICAL JOURNAL
SPECIAL TOPICS

Detecting chaos, determining the dimensions of tori and predicting slow diffusion in Fermi–Pasta–Ulam lattices by the Generalized Alignment Index method

C. Skokos[1,a], T. Bountis[2,b], and C. Antonopoulos[2,c]

[1] Astronomie et Systèmes Dynamiques, IMCCE, Observatoire de Paris, 77 avenue Denfert-Rochereau, 75014 Paris, France
[2] Department of Mathematics, Division of Applied Analysis and Center for Research and Applications of Nonlinear Systems (CRANS), University of Patras, 26500 Patras, Greece

Abstract. The recently introduced GALI method is used for rapidly detecting chaos, determining the dimensionality of regular motion and predicting slow diffusion in multi-dimensional Hamiltonian systems. We propose an efficient computation of the $GALI_k$ indices, which represent volume elements of k randomly chosen deviation vectors from a given orbit, based on the Singular Value Decomposition (SVD) algorithm. We obtain theoretically and verify numerically asymptotic estimates of GALIs long-time behavior in the case of regular orbits lying on low-dimensional tori. The $GALI_k$ indices are applied to rapidly detect chaotic oscillations, identify low-dimensional tori of Fermi–Pasta–Ulam (FPU) lattices at low energies and predict weak diffusion away from quasiperiodic motion, long before it is actually observed in the oscillations.

1 Introduction

A great variety of physical systems can be described by Hamiltonian systems or symplectic maps [1–3]. Their applications range from the stability of the solar system [4] and the containment of charged particles in high intensity magnetic fields [3] to the blow-up of hadron beams in high energy accelerators [5] and the study of simple molecules and hydrogen-bonded systems [6,7]. More recently, much attention has been focused on the dynamics of nonlinear lattices and in particular on localization in the form of q-breathers [8] energy transport and equipartition properties of Fermi–Pasta–Ulam (FPU) particle chains [9]. The main difficulty with determining the nature of the motion in Hamiltonian dynamics is that regular and chaotic orbits are distributed in phase space in very intricate ways, in contrast with dissipative systems, where all orbits eventually fall on regular or chaotic attractors.

The most widely used method for distinguishing order from chaos in dynamical systems is the evaluation of the Lyapunov Exponents (LEs) σ_i for each given orbit. Benettin et al. [10] studied the problem of determining all LEs theoretically and proposed in [11] an algorithm for their numerical computation. In practice, one often calculates only the largest LE, σ_1, following one deviation vector from the given orbit and if $\sigma_1 > 0$ the orbit is characterized as chaotic.

In the present paper, we apply the Generalized ALignment Index of order k, $GALI_k$, $k = 2, \ldots, 2N$ [12], to distinguish efficiently between regular and chaotic orbits of multi-dimensional

[a] e-mail: hskokos@imcce.fr
[b] e-mail: bountis@math.upatras.gr
[c] e-mail: antonop@math.upatras.gr

Hamiltonian systems of N degrees of freedom. These indices generalize a similar indicator called Smaller ALignment Index (SALI) [13], in that they use information of *more than two* deviation vectors from the reference orbit (see [12] for more details). In particular, the GALI_k is proportional to volume elements formed by k initially linearly independent unit deviation vectors whose magnitude is normalized to unity at every time step.

After recalling briefly the definition of GALI_k and its general behavior for regular and chaotic motion in section 2.1, we propose in section 2.2 a technique for the efficient computation of GALI_k, based on the Singular Value Decomposition (SVD) of the matrix having as rows the k normalized deviation vectors. In section 2.3 we study theoretically the behavior of GALIs for regular orbits of N degrees of freedom Hamiltonian systems that lie on an s-dimensional torus, with $2 \leq s \leq N$. In section 3 we present applications of the GALI_k approach to an $N = 8$ particles FPU lattice and show that the GALI_k indices: (i) can be used for the rapid discrimination between regular and chaotic motion, (ii) determine the correct dimensionality of tori and (iii) predict that the motion is weakly chaotic, long before this can be seen in the actual oscillations.

By 'weak chaos' we mean weakly diffusive motion through a network of resonances. On the other hand, when one speaks of 'sticky' orbits [14], one generally refers to motion occurring just outside the boundary of a large regular region, where orbits remain for a long times before rapidly escaping to distant parts of phase space through a large chaotic sea. In our case, 'weakly chaotic' motion occurs within regimes 'surrounded' by (often high-dimensional) tori, is characterized by very small LEs and is reminiscent of what is called in the literature Arnol'd diffusion [3]. Finally, in section 4, we summarize the results and present our conclusions.

2 The GALI method

2.1 Definition and behavior of GALI

Following [12] let us first briefly recall the definition of GALI and its behavior for regular and chaotic motion. We consider a Hamiltonian system of N degrees of freedom having a Hamiltonian $H(q_1, \ldots, q_N, p_1, \ldots, p_N)$ where q_i and p_i, $i = 1, \ldots, N$ are the generalized coordinates and momenta respectively. An orbit of this system is defined by a vector $\mathbf{x}(t) = (x_1(t), \ldots, x_{2N}(t))$, with $x_i = q_i$, $x_{i+N} = p_i$, $i = 1, \ldots, N$. This orbit is a solution of Hamilton's equations $d\mathbf{x}/dt = \mathcal{V}(\mathbf{x}) = (\partial H/\partial \mathbf{p}, -\partial H/\partial \mathbf{q})$, while the evolution of a deviation vector $\mathbf{w}(t)$ from $\mathbf{x}(t)$ obeys the variational equations $d\mathbf{w}/dt = \mathbf{M}(\mathbf{x}(t))\,\mathbf{w}$, where $\mathbf{M} = \partial \mathcal{V}/\partial \mathbf{x}$ is the Jacobian matrix of $\mathcal{V}$.

Let us follow k normalized deviation vectors $\hat{w}_1, \ldots, \hat{w}_k$ (with $2 \leq k \leq 2N$) in time, and determine whether they become linearly dependent, by checking if the volume of the corresponding k-parallelogram goes to zero. This volume is equal to the norm of the wedge or exterior product [15] of these vectors. Hence we are led to define the following 'volume' element:

$$\mathrm{GALI}_k(t) = \|\hat{w}_1(t) \wedge \hat{w}_2(t) \wedge \cdots \wedge \hat{w}_k(t)\|, \tag{1}$$

which we call the Generalized Alignment Index (GALI) of order k. We note that the hat ($\hat{}$) over a vector denotes that it is of unit magnitude. Thus, for each initial condition $\mathbf{x}(0)$, we solve Hamilton's equations for $\mathbf{x}(t)$, together with their variational equations for k initially linearly independent deviation vectors $\hat{w}_i$, $i = 1, \ldots, k$. Clearly, if at least two of these vectors become linearly dependent, the wedge product in (1) becomes zero and the volume element vanishes.

In the case of a chaotic orbit all deviation vectors tend to become linearly dependent, aligning in the direction of the eigenvector which corresponds to the maximal Lyapunov exponent and GALI_k tends to zero exponentially following the law [12]:

$$\mathrm{GALI}_k(t) \sim e^{-[(\sigma_1-\sigma_2)+(\sigma_1-\sigma_3)+\cdots+(\sigma_1-\sigma_k)]t}, \tag{2}$$

where $\sigma_1, \ldots, \sigma_k$ are approximations of the first k largest Lyapunov exponents. In the case of regular motion on the other hand, all deviation vectors tend to fall on the N-dimensional

tangent space of the torus on which the motion lies. Thus, if we start with $k \leq N$ general deviation vectors they will remain linearly independent on the N-dimensional tangent space of the torus, since there is no particular reason for them to become aligned. As a consequence GALI_k remains practically constant for $k \leq N$. On the other hand, GALI_k tends to zero for $k > N$, since some deviation vectors will eventually become linearly dependent, following a particular power law which depends on the dimensionality N of the torus and the number k of deviation vectors. So, the generic behavior of GALI_k for regular orbits lying on N-dimensional tori is given by [12]:

$$\mathrm{GALI}_k(t) \sim \begin{cases} \text{constant} & \text{if } 2 \leq k \leq N \\ \frac{1}{t^{2(k-N)}} & \text{if } N < k \leq 2N. \end{cases} \tag{3}$$

2.2 Numerical computation of GALI

In order to numerically compute GALI_k in [12] using (1) we considered as a basis of the $2N$-dimensional tangent space of the Hamiltonian flow the usual set of orthonormal vectors $\hat{e}_1 = (1, 0, 0, \ldots, 0)$, $\hat{e}_2 = (0, 1, 0, \ldots, 0), \ldots, \hat{e}_{2N} = (0, 0, 0, \ldots, 1)$. So, any unitary deviation vector $\hat{w}_i$ can be written as:

$$\hat{w}_i = \sum_{j=1}^{2N} w_{ij} \hat{e}_j, \qquad i = 1, 2, \ldots, k \tag{4}$$

where w_{ij} are real numbers satisfying $\sum_{j=1}^{2N} w_{ij}^2 = 1$. Considering the $k \times 2N$ matrix $\mathbf{A}$ having as rows the coordinates of k such vectors, we can write equations (4) in matrix form as:

$$\begin{bmatrix} \hat{w}_1 \\ \hat{w}_2 \\ \vdots \\ \hat{w}_k \end{bmatrix} = \begin{bmatrix} w_{11} & w_{12} & \cdots & w_{1\,2N} \\ w_{21} & w_{22} & \cdots & w_{2\,2N} \\ \vdots & \vdots & & \vdots \\ w_{k1} & w_{k2} & \cdots & w_{k\,2N} \end{bmatrix} \cdot \begin{bmatrix} \hat{e}_1 \\ \hat{e}_2 \\ \vdots \\ \hat{e}_{2N} \end{bmatrix} = \mathbf{A} \cdot \begin{bmatrix} \hat{e}_1 \\ \hat{e}_2 \\ \vdots \\ \hat{e}_{2N} \end{bmatrix}. \tag{5}$$

The norm of the wedge product of the k deviation vectors appearing in (1) was defined in [12] as the square root of the sum of the squares of the determinants of all possible $k \times k$ submatrices of matrix $\mathbf{A}$. So, for the computation of GALI_k we have:

$$\mathrm{GALI}_k = \|\hat{w}_1 \wedge \hat{w}_2 \wedge \cdots \wedge \hat{w}_k\| = \left\{ \sum_{1 \leq i_1 < i_2 < \cdots < i_k \leq 2N} \left(\det \begin{bmatrix} w_{1i_1} & w_{1i_2} & \cdots & w_{1i_k} \\ w_{2i_1} & w_{2i_2} & \cdots & w_{2i_k} \\ \vdots & \vdots & & \vdots \\ w_{ki_1} & w_{ki_2} & \cdots & w_{ki_k} \end{bmatrix} \right)^2 \right\}^{1/2}, \tag{6}$$

where the sum is performed over all possible combinations of k indices out of $2N$.

Equation (6) is ideal for the theoretical determination of the asymptotic (long time) behavior of GALIs for chaotic and regular orbits (see [12] for more details), as well as, for regular orbits that lie on low dimensional tori (see section 2.3 below). However, from a practical point of view the computation of determinants is not the most efficient way of computing GALI_k, as has already pointed out in [16]. For low dimensional systems, the number of determinants appearing in (6) for the computation of GALI_k is not prohibitive, but as the number of degrees of freedom increases the computation can become extremely time consuming and in some cases impractical. For example, in the case of an $N = 8$ degree of freedom system, like the one studied in section 3, the computation of GALI_8 requires the evaluation of 12870 8×8 determinants, while, GALI_{15} in an $N = 15$ degree of freedom system requires the computation of 155117520 15×15 determinants!

We have already mentioned that GALI_k measures the volume of the k-parallelogram P_k having as edges the k unitary deviation vectors $\hat{w}_i$, $i = 1, \ldots, k$ of (4) and (5) above. The volume of P_k is then given by (see for instance [17]):

$$\mathrm{vol}(P_k) = \sqrt{\det(\mathbf{A} \cdot \mathbf{A}^{\mathrm{T}})}, \tag{7}$$

where $(^{\mathrm{T}})$ denotes transpose. Since $\det(\mathbf{A} \cdot \mathbf{A}^{\mathrm{T}})$ is equal to the sum appearing in (6) (this equality is called Lagrange's identity, see for instance [18]), we have:

$$\mathrm{GALI}_k = \sqrt{\det(\mathbf{A} \cdot \mathbf{A}^{\mathrm{T}})}, \tag{8}$$

as an alternative way of computing GALI_k, where only the multiplication of two matrices and the square root of one determinant appears.

A different way of evaluating GALI_k, which actually proved to be more accurate, is obtained by performing the Singular Value Decomposition (SVD) of $\mathbf{A}^{\mathrm{T}}$. So, the $2N \times k$ matrix $\mathbf{A}^{\mathrm{T}}$ can be written as the product of a $2N \times k$ column-orthogonal matrix $\mathbf{U}$, a $k \times k$ diagonal matrix $\mathbf{Z}$ with positive or zero elements z_i, $i = 1, \ldots, k$ (the so-called *singular values*), and the transpose of a $k \times k$ orthogonal matrix $\mathbf{V}$:

$$\mathbf{A}^{\mathrm{T}} = \mathbf{U} \cdot \mathbf{Z} \cdot \mathbf{V}^{\mathrm{T}}. \tag{9}$$

We note that matrices $\mathbf{U}$ and $\mathbf{V}$ are orthogonal so that:

$$\mathbf{U}^{\mathrm{T}} \cdot \mathbf{U} = \mathbf{V}^{\mathrm{T}} \cdot \mathbf{V} = \mathrm{I}_k, \tag{10}$$

with I_k being the $k \times k$ unit matrix. For a more detailed description of the SVD method, as well as an algorithm for its implementation the reader is referred to [19] and references therein. Using Eq. (8) for the computation of GALI_k, as well as Eqs. (9) and (10), we get:

$$\begin{aligned} \mathrm{GALI}_k &= \sqrt{\det\left(\mathbf{A} \cdot \mathbf{A}^{\mathrm{T}}\right)} = \sqrt{\det\left(\mathbf{V} \cdot \mathbf{Z}^{\mathrm{T}} \cdot \mathbf{U}^{\mathrm{T}} \cdot \mathbf{U} \cdot \mathbf{Z} \cdot \mathbf{V}^{\mathrm{T}}\right)} \\ &= \sqrt{\det\left(\mathbf{V} \cdot \mathrm{diag}(z_i^2) \cdot \mathbf{V}^{\mathrm{T}}\right)} = \sqrt{\det\left(\mathrm{diag}(z_i^2)\right)} = \prod_{i=1}^{k} z_i. \end{aligned}$$

Thus, we conclude that GALI_k is equal to the product of the singular values of matrix $\mathbf{A}$ (5) defined by the k normalized deviation vectors and at the same time, we theoretically explain the computationally verified equality of this product to values of GALI_k computed by (6) which was reported in [16]. The SVD approach, therefore, provides a very accurate determination of the logarithm of GALI_k, which can now be used for the discrimination between regular and chaotic motion, as it leads to:

$$\log(\mathrm{GALI}_k) = \sum_{i=1}^{k} \log(z_i), \tag{11}$$

and for this reason we implement this approach for the computation of GALI_k in numerical applications. From Eq. (11) we see that the computation of the singular values z_i with the usual double precision accuracy, permits the accurate determination of large negative values of $\log(\mathrm{GALI}_k)$, which correspond to very small values of GALI_k.

The problem of the numerical computation of orbits, keeping constant the numerical value of the Hamiltonian H, is of great importance in numerical studies of dynamical systems. Several integration schemes have been developed and applied over the years with varying degrees of success (see [20] for a survey of such methods). In our study we use an 8th order Runge–Kutta method proposed in [21], both for the numerical integration of Hamilton's equations (evolution of an orbit), as well as for the variational equations (evolution of deviation vectors). The scheme proved to be very efficient and accurate since, in all our computations, we always kept the relative error of the values of the Hamiltonian function ($|H(t) - H(0)|/|H(0)|$) below 10^{-12}.

2.3 Behavior of GALI for regular orbits of low dimensional tori

Now we turn to the GALI$_k$ method for regular orbits of an N degree of freedom Hamiltonian, that lie on s-dimensional tori, with $2 \leq s \leq N$. In this case, one could perform a local transformation to action-angle variables, J_i, θ_i, whence Hamilton's equations of motion can be easily integrated to give $J_i(t) = J_{i0}$, $\theta_i(t) = \theta_{i0} + \omega_i(J_{10}, \ldots, J_{s0})t$, where J_{i0}, θ_{i0} are the initial conditions ($i = 1, \ldots, N$) and $\omega_i \equiv 0$ for $s < i \leq N$. Denoting by ξ_i, η_i small deviations from the J_i and θ_i respectively and using as basis of the $2N$-dimensional tangent space of the Hamiltonian flow the $2N$ unit vectors $\{\hat{v}_1, \ldots, \hat{v}_{2N}\}$, such that the first N of them correspond to the N action variables and the remaining ones to the N conjugate angle variables, any deviation vector $\mathbf{w}_i$, $i = 1, 2, \ldots$ can be written as

$$\boldsymbol{w}_i(t) = \sum_{j=1}^{N} \xi_j^i(0)\hat{v}_j + \sum_{j=1}^{N} \left(\eta_j^i(0) + \sum_{k=1}^{N} \omega_{jk}\xi_k^i(0)t \right) \hat{v}_{N+j}, \tag{12}$$

with $\omega_{kj} = \partial\omega_k/\partial J_j$ computed from the initial values J_{j0} for $k, j = 1, 2, \ldots, s$ and $\omega_{kj} \equiv 0$ for $k, j = s+1, s+2, \ldots, N$. It follows easily from the above that for sufficiently long times, $\|\mathbf{w}(t)\| \sim t$.

Let us now study the case of k, initially linearly independent, randomly chosen, unit deviation vectors $\{\hat{w}_1, \ldots, \hat{w}_k\}$ expressed in terms of the new basis by the transformation $[\hat{w}_1 \ldots \hat{w}_k]^{\mathrm{T}} = \mathbf{D} \cdot [\hat{v}_1 \ldots \hat{v}_{2N}]^{\mathrm{T}}$. The random choice of the initial deviation vectors corresponds to the generic (most probable) configuration that none of them lies in the tangent space of the torus. In the opposite case, the results do not change qualitatively since GALI$_k$ still exhibit power law decays, but with slightly different exponents [12]. Defining by $\boldsymbol{\xi}_i^k$ and $\boldsymbol{\eta}_i^k$ the $k \times 1$ column matrices of initial conditions, the matrix $\mathbf{D}$ assumes the form

$$\mathbf{D}(t) \sim \frac{1}{t^k} \cdot \mathbf{D}^k(t) = \frac{1}{t^k} \left[\boldsymbol{\xi}_1^k \ldots \boldsymbol{\xi}_N^k \; \boldsymbol{\eta}_1^k + \textstyle\sum_{i=1}^{s} \omega_{1i}\boldsymbol{\xi}_i^k t \ldots \boldsymbol{\eta}_s^k + \sum_{i=1}^{s} \omega_{si}\boldsymbol{\xi}_i^k t \; \boldsymbol{\eta}_{s+1}^k \ldots \boldsymbol{\eta}_N^k \right], \tag{13}$$

where we have replaced the first factor on the right by its asymptotic expression for long times.

In the case of an s-dimensional torus, the k deviation vectors eventually fall on its s-dimensional tangent space spanned by $\hat{v}_{N+1}, \ldots, \hat{v}_{N+s}$. If we start with $2 \leq k \leq s$ deviation vectors, since there is no reason for them to become linearly dependent, their wedge product yields GALI$_k$ indices that are different from zero. However, if we start with $s < k \leq 2N$ deviation vectors, some of them will necessarily become linearly dependent and thus their wedge product (as well as the GALI$_k$) will tend to zero not exponentially but by *a power law*, as we explain below.

In order to determine the leading order behavior of the GALI$_k$, we search for the fastest increasing determinants of all $k \times k$ minors of the matrix $\mathbf{D}^k$, as t grows. For $2 \leq k \leq s$, these determinants have k columns chosen among the s columns of matrix $\mathbf{D}^k$ with $\omega_{ij} \neq 0$ and grow as t^k, thus providing constant terms to the GALI$_k$. All other determinants contain at least one column from the $2N - s$ time independent columns of matrix $\mathbf{D}^k$ and introduce terms that grow *slower* than t^k, having ultimately no bearing on the behavior of GALI$_k(t)$. This yields the important result that GALI$_k(t) \sim$ constant for $2 \leq k \leq s$.

Next, we turn to the case of $s < k \leq 2N - s$. The fastest growing determinants are again those containing the s columns of the matrix $\mathbf{D}^k$ with $\omega_{ij} \neq 0$. The remaining $k - s$ columns are chosen among the $2(N - s)$ columns of $\mathbf{D}^k$ which are time independent (excluding the $\boldsymbol{\xi}_i^k$ columns with $i \leq s$). Among these determinants, the fastest increasing ones are those containing as many columns proportional to t as possible. Thus, t appears at most s times and the time evolution of GALI$_k$ is mainly determined by terms proportional to $t^s/t^k = 1/t^{(k-s)}$ and hence GALI$_k(t) \sim t^{(s-k)}$ for $s < k \leq 2N - s$.

Finally, let us consider the behavior of GALI$_k$ when $2N - s < k \leq 2N$. Again the fastest growing determinants contain the s columns of $\mathbf{D}^k$ with $\omega_{ij} \neq 0$, while the rest $k - s$ columns are chosen among the remaining $k - s$ time independent columns of $\mathbf{D}^k$. In order to have as many columns proportional to t as possible these determinants should contain

$k-(2N-s)=k+s-2N$ columns among the $\boldsymbol{\xi}_i^k$ columns with $i \leq s$, as well as the corresponding $\boldsymbol{\eta}_i^k$ columns. Thus, t appears at most $s-(k+s-2N)=2N-k$ times and the time evolution of GALI_k is determined by terms proportional to $t^{2N-k}/t^k = 1/t^{2(k-N)}$. Summarizing, we have shown that the GALI_k for regular orbits lying on an s-dimensional torus behave as [22]:

$$\mathrm{GALI}_k(t) \sim \begin{cases} \text{constant} & \text{if} \quad 2 \leq k \leq s, \\ \frac{1}{t^{k-s}} & \text{if} \quad s < k \leq 2N-s, \\ \frac{1}{t^{2(k-N)}} & \text{if} \quad 2N-s < k \leq 2N. \end{cases} \tag{14}$$

Note that from (14) we deduce that for $s=N$, GALI_k remains constant for $2 \leq k \leq N$ and decreases to zero as $\sim 1/t^{2(k-N)}$ for $N < k \leq 2N$ in accordance with (3).

3 Applications

We now apply the GALI method to study chaotic, quasiperiodic and diffusive motion in multi-dimensional Hamiltonian systems. In particular, we consider the FPU β-lattice of N particles with Hamiltonian [8,9]

$$H = \sum_{i=1}^{N} \frac{p_i^2}{2} + \sum_{i=0}^{N} \left[\frac{(q_{i+1}-q_i)^2}{2} + \frac{\beta (q_{i+1}-q_i)^4}{4} \right], \tag{15}$$

with $q_1, \ldots, q_N$ being the displacements of the particles with respect to their equilibrium positions, and $p_1, \ldots, p_N$ the corresponding momenta. It is well known that if we define normal mode variables by

$$Q_k = \sqrt{\frac{2}{N+1}} \sum_{i=1}^{N} q_i \sin\left(\frac{ki\pi}{N+1}\right), \qquad P_k = \sqrt{\frac{2}{N+1}} \sum_{i=1}^{N} p_i \sin\left(\frac{ki\pi}{N+1}\right), \qquad k=1,\ldots,N, \tag{16}$$

the unperturbed Hamiltonian (equation (15) for $\beta=0$) is written as the sum of the so-called *harmonic energies* E_i having the form:

$$E_i = \frac{1}{2}\left(P_i^2 + \omega_i^2 Q_i^2\right), \qquad \omega_i = 2\sin\left(\frac{i\pi}{2(N+1)}\right), \quad i=1,\ldots,N, \tag{17}$$

with ω_i being the corresponding *harmonic frequencies*. In our study we impose fixed boundary conditions $q_0(t)=q_{N+1}(t)=p_0(t)=p_{N+1}(t)=0$, $\forall t$ and fix the number of particles to $N=8$ and the system's parameter to $\beta=1.5$.

We consider first a chaotic orbit of (15), having seven positive Lyapunov exponents, which we compute as the limits for $t \to \infty$ of some appropriate quantities L_i, $i=1,\ldots,7$ (see [11] for more details), to be $\sigma_1 \approx 0.170$, $\sigma_2 \approx 0.141$, $\sigma_3 \approx 0.114$, $\sigma_4 \approx 0.089$, $\sigma_5 \approx 0.064$, $\sigma_6 \approx 0.042$, $\sigma_7 \approx 0.020$ (Fig. 1(a)). We recall that chaotic orbits of Hamiltonian systems possess Lyapunov exponents which are real and grouped in pairs of opposite sign, with two of them being equal to zero. We, therefore, have in the case of the $N=8$ particle FPU lattice (15) $\sigma_i = -\sigma_{17-i}$ for $i=1,\ldots,8$ with $\sigma_8=\sigma_9=0$. Using the above computed values as good approximations of the real Lyapunov exponents, we see in Figs. 1(b) and 1(c) that the slopes of all GALI_k indices are well reproduced by (2).

Turning now to the case of a regular orbit of (15), we plot in Fig. 2(a) the evolution of its harmonic energies E_i, $i=1,\ldots,8$. The harmonic energies remain practically constant, exhibiting some feeble oscillations, implying the regular nature of the orbit. In Figs. 2(b) and 2(c) we plot the GALIs of this orbit and verify that their behavior is well approximated by the asymptotic formula (3) for $N=8$. Note that the GALI_k for $k=2,\ldots,8$ (Fig. 2(b)) remain different from zero implying that the orbit is indeed quasiperiodic and lies on a 8-dimensional torus. In particular, after some initial transient time, they start oscillating around non-zero

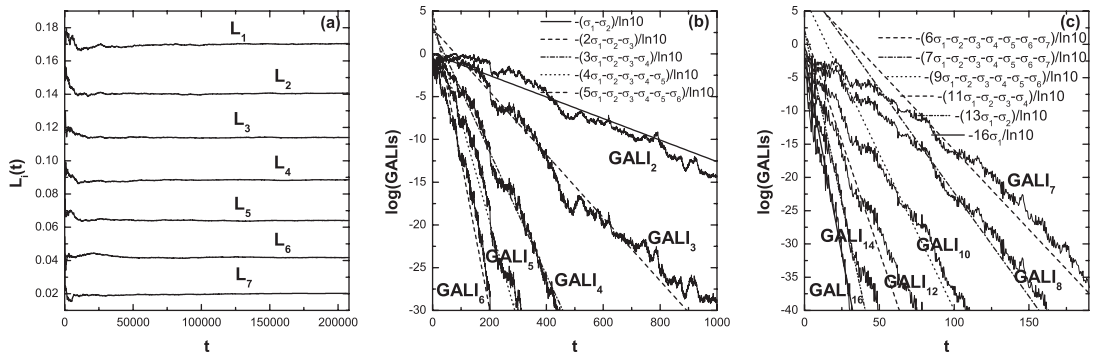

Fig. 1. (a) The time evolution of quantities L_i, $i = 1, \ldots, 7$, having as limits for $t \to \infty$ the seven positive Lyapunov exponents σ_i, $i = 1, \ldots, 7$, for a chaotic orbit with initial conditions $Q_1 = Q_4 = 2$, $Q_2 = Q_5 = 1$, $Q_3 = Q_6 = 0.5$, $Q_7 = Q_8 = 0.1$, $P_i = 0$, $i = 1, \ldots, 8$ of the $N = 8$ particle FPU lattice (15). The time evolution of the corresponding GALI_k is plotted in (b) for $k = 2, \ldots, 6$ and in (c) for $k = 7, 8, 10, 12, 14, 16$. The plotted lines in (b) and (c) correspond to exponentials that follow the asymptotic laws (2) for $\sigma_1 = 0.170$, $\sigma_2 = 0.141$, $\sigma_3 = 0.114$, $\sigma_4 = 0.089$, $\sigma_5 = 0.064$, $\sigma_6 = 0.042$, $\sigma_7 = 0.020$. Note that t-axis is linear and that the slope of each line is written explicitly in (b) and (c).

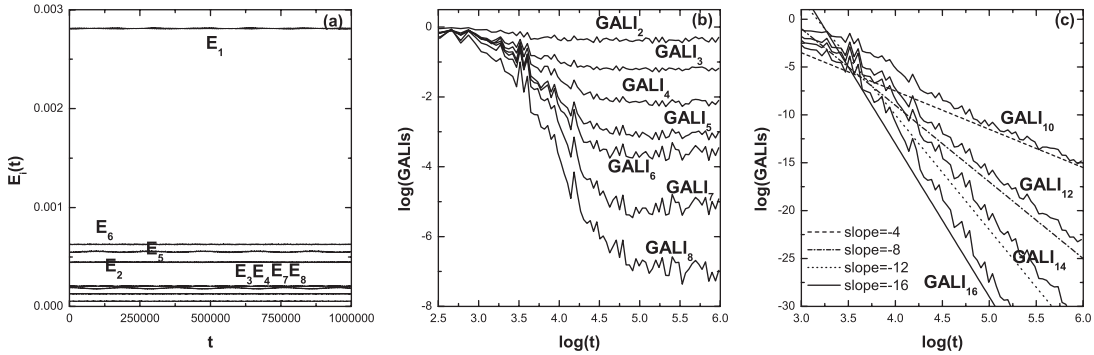

Fig. 2. (a) The time evolution of harmonic energies E_i, $i = 1, \ldots, 8$, for a regular orbit with initial conditions $q_1 = q_2 = q_3 = q_8 = 0.05$, $q_4 = q_5 = q_6 = q_7 = 0.1$, $p_i = 0$, $i = 1, \ldots, 8$ of the $N = 8$ particle FPU lattice (15). The time evolution of the corresponding GALI_k is plotted in (b) for $k = 2, \ldots, 8$ and in (c) for $k = 10, 12, 14, 16$. The plotted lines in (c) correspond to functions proportional to t^{-4}, t^{-8}, t^{-12} and t^{-16}, as predicted in (3).

values whose magnitude decreases with increasing k. On the other hand, the GALI_k with $8 < k \leq 16$ (Fig. 2(c)) tend to zero following power law decays in accordance to (3).

From the results of Figs. 1 and 2, we conclude that the different behavior of GALI_k for chaotic (exponential decay) and regular orbits (non-zero values or power law decay) allows for a fast and clear discrimination between the two cases. Let us consider for example GALI_8 which tends exponentially to zero for chaotic orbits (Fig. 1(c)), while it remains small but different from zero in the case of regular orbits (Fig. 2(b)). At $t \approx 150$ GALI_8 has values that differ almost 35 orders of magnitude being $\mathrm{GALI}_8 \approx 10^{-36}$ for the chaotic orbit, while $\mathrm{GALI}_8 \approx 10^{-1}$ for the regular one. This huge difference in the values of GALI_8 clearly identifies the chaotic nature of the orbit.

If we select initial conditions such that only a small number of the harmonic energies E_i are initially excited, we observe, at small enough energies that (15) exhibits the famous FPU recurrences, whereby energy is exchanged quasiperiodically only between the excited E_is.

In Fig. 3, we consider the case of a regular orbit with initial conditions $Q_1 = 2$, $P_1 = 0$, $Q_i = P_i = 0$, $i = 2, \ldots, 8$ having total energy $H = 0.24$. In Fig. 3(a) we see that only two normal modes are exited, namely E_1 and E_3, while all other harmonic energies remain practically zero. Observe that among the GALI_k plotted in Figs. 3(b) and (c), only $\mathrm{GALI}_2 \approx$ const., indicating

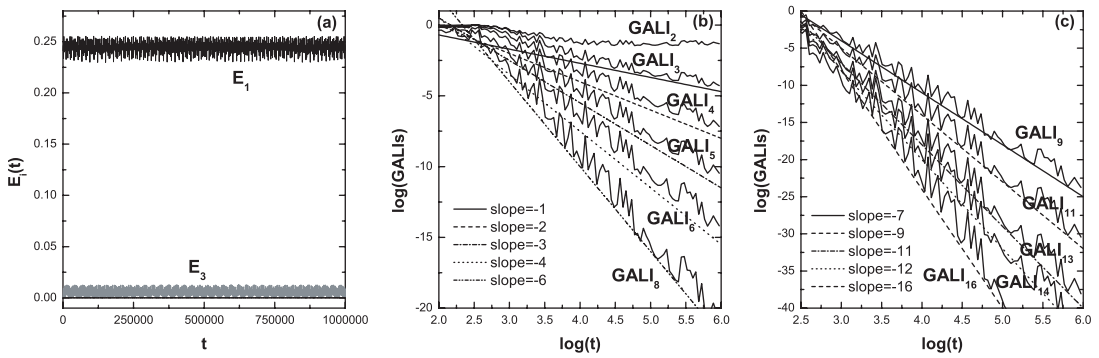

Fig. 3. (a) The time evolution of harmonic energies for a regular orbit lying on a 2-dimensional torus of the $N = 8$ particle FPU lattice (15). Recurrences occur between E_1 and E_3, while all other harmonic energies remain practically zero. The time evolution of the corresponding GALI_k is plotted in (b) for $k = 2, \ldots, 6, 8$ and in (c) for $k = 9, 11, 13, 14, 16$. The plotted lines in (b) and (c) correspond to precisely the power laws predicted in (14).

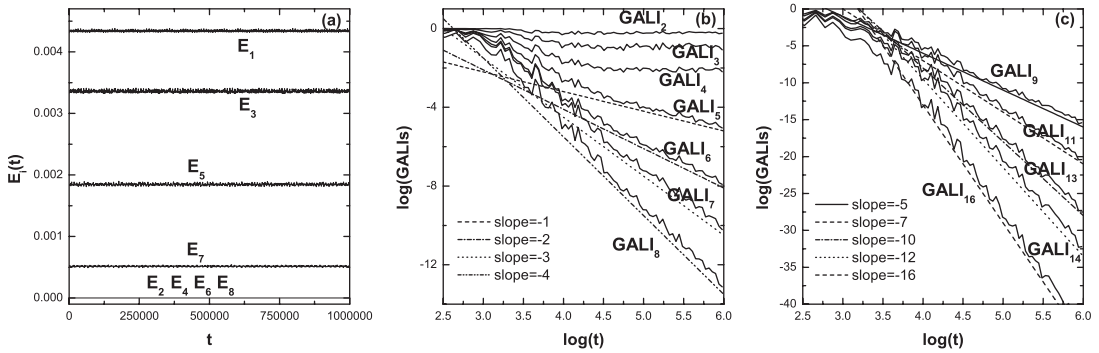

Fig. 4. (a) The time evolution of harmonic energies for a regular orbit lying on a 4-dimensional torus of the $N = 8$ particle FPU lattice (15). Recurrences occur between E_1, E_3, E_5 and E_7, while all other harmonic energies remain practically zero. The time evolution of the corresponding GALI_k is plotted in (b) for $k = 2, \ldots, 8$ and in (c) for $k = 9, 11, 13, 14, 16$. The plotted lines in (b) and (c) correspond to the precise power laws predicted in (14).

that the torus is only 2-dimensional, while all others decay by power laws whose exponents are the ones given in (14) for $N = 8$ and $s = 2$ (see also [22] for more details).

Let us now choose initial conditions so as to distribute the energy among 4 modes, E_i, $i = 1, 3, 5, 7$, in our 8-particle FPU lattice. In particular, we consider an orbit with initial conditions $q_i = 0.1$, $p_i = 0$, $i = 1, \ldots, 8$, having total energy $H = 0.01$. What we observe again is that since only these 4 modes are excited (Fig. 4(a)), only the GALI_k for $k = 2, 3, 4$ remain constant (Fig. 4(b)), implying that the motion lies on a 4-dimensional torus, while all the higher order GALIs decay by power laws, whose exponents are derived in (14) for $N = 8$ and $s = 4$.

What happens, however, if we choose an orbit that starts near a torus but slowly drifts away from it, presumably through a thin chaotic layer of higher order resonances? This phenomenon is recognized by the GALIs, which provide early predictions that may be quite relevant for applications. To see this let us choose again initial conditions for our 8-particle FPU lattice, such that the motion appears quasiperiodic, with its energy recurring between the modes E_1, E_3, E_5 and E_7 (Fig. 5(a)). In particular, we consider an orbit with initial conditions $Q_1 = 2$, $Q_7 = 0.44$, $Q_3 = Q_4 = Q_5 = Q_6 = Q_8 = 0$, $P_i = 0$, $i = 1, \ldots, 8$, having total energy $H = 0.71$. This orbit, however, is *not* quasiperiodic, as it drifts away from the initial 4-dimensional torus, exciting new frequencies and sharing its energy with more modes, after about $t = 20000$ time units. This becomes evident in Fig. 5(b) where we plot the evolution of E_6 and E_8. We see that these harmonic energies, which were initially zero, start having non-zero values at $t \approx 20000$ and

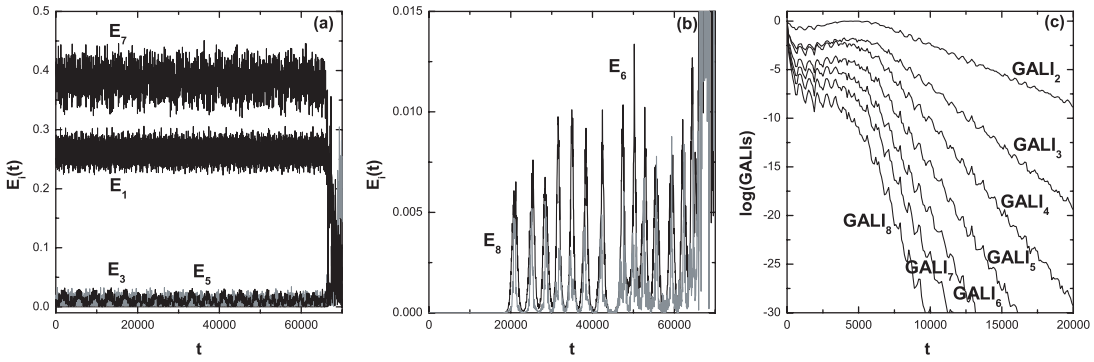

Fig. 5. The time evolution of harmonic energies (a) E_1, E_3, E_5, E_7 and (b) E_6, E_8, for a slowly diffusing orbit of the $N = 8$ particle FPU lattice (15). (c) The time evolution of the corresponding GALI_k for $k = 2, \ldots, 8$, clearly exhibits exponential decay already at $t \approx 10000$.

exhibit from then on small oscillations (note the different scales of ordinate axis of Figs. 5(a) and (b)), which look very regular until $t \approx 66000$. At that time the values of all harmonic energies change dramatically, clearly indicating the chaotic nature of the orbit. As we see in Fig. 5(c), this type of diffusion is predicted by the *exponential* decay of *all* GALI_k, shown already at about $t = 10000$.

4 Summary

We have applied the Generalized Alignment Index of order k (GALI_k) as a tool for studying the dynamics in conservative dynamical systems, and in particular in Hamiltonian systems of N degrees of freedom. We have shown that these indices not only distinguish rapidly between chaotic and regular orbits, but also determine the dimensionality of quasiperiodic tori and detect slow diffusion away from quasiperiodicity, long before this becomes evident in the dynamics.

The GALI_k represents the 'volume' of a generalized parallelogram having as edges $k > 2$ initially linearly independent unit deviation vectors and are computed as the norm of the wedge product of these vectors. We verified numerically that for chaotic orbits GALI_k tends exponentially to zero following a rate which depends on the values of several Lyapunov exponents (see Eq. (2)). In the case of regular orbits lying on N-dimensional tori, GALI_k with $2 \leq k \leq N$ eventually fluctuates around non-zero values, while for $N < k \leq 2N$, it tends to zero following a particular power law (see Eq. (3)). If, on the other hand, the orbit lies on an s-dimensional torus, with $2 \leq s \leq N$, we showed analytically and verified numerically that GALI_k is nearly constant for $2 \leq k \leq s$ and, if $s < k \leq 2N$, decays as a power law, the precise form of which depends on the dimensionality of the torus (see Eq. (14)).

Computationally, of course, it is somewhat costly to evaluate the large number of determinants needed to obtain the GALI_ks by Eq. (6), especially in the case of large N. As a solution to this problem, we introduced and theoretically explained in section 2.2 an efficient and accurate method of computing $\log(\mathrm{GALI}_k)$ by applying the technique of Singular Value Decomposition (SVD) to the matrix of deviation vectors and evaluating the product of its singular values (see Eq. (11)).

Applying next the GALI method to a 1-dimensional Fermi–Pasta–Ulam (FPU) lattice of $N = 8$ particles, we have demonstrated that GALIs do answer efficiently and reliably some fundamental questions of practical concern: When is the motion quasiperiodic and what is the dimensionality of the torus on which it lies? This is quite important when one wishes to determine the number of frequencies involved and leads to the interesting result that the dimension can be much less than the generally expected number of degrees of freedom N. Also, when is the motion *not quasiperiodic* but diffuses slowly away from a torus through a chaotic network of higher order resonances? This is notoriously difficult to ascertain (especially for

large N), as the dynamics is 'sticky', Lyapunov exponents may be very small and thus long integrations are needed before the chaotic nature of the motion becomes evident.

We believe that the results we have presented on the FPU lattice demonstrate that the GALI$_k$ method can prove very useful to many practical applications: In celestial mechanics, there are many higher dimensional N-body problems [4,23], where one would like to locate invariant tori and determine the extent of phase space occupied by regular and chaotic orbits. In chemical dynamics, small molecules have been recently studied whose properties depend on the presence of stable oscillatory modes carrying large regions of quasiperiodic motion about them [7]. Many interesting problems are also described by N-dimensional symplectic maps, as e.g. in accelerator dynamics, where the presence of large regions of tori is essential for maximizing the stability of betatron oscillations [5].

Ch.S. was supported by the Marie Curie Intra-European Fellowship No. MEIF-CT-2006-025678. This work was partially supported by the European Social Fund (ESF), Operational Program for Educational and Vocational Training II (EPEAEK II) and particularly the Program PYTHAGORAS II. We would also like to thank both referees for their remarks.

References

1. B.V. Chirikov, Phys. Rep. **180**, 179 (1979)
2. R.S. MacKay, J.D. Meiss, *Hamiltonian Dynamical Systems* (Adam Hilger, Bristol, 1987)
3. M.A. Lieberman, A.J. Lichtenberg, *Regular and Chaotic Dynamics* (Springer Verlag, 1992)
4. G. Contopoulos, *Order and Chaos in Dynamical Astronomy* (Springer, Berlin, 2002)
5. *Nonlinear Problems in Future Particle Accelerators*, edited by W. Scandale, G. Turchetti (World Scientific, Singapore, 1991); T. Bountis, Ch. Skokos, Nucl. Instrum. Meth. Res. A **561**, 173 (2006)
6. S.C. Farantos, Z.-W. Qu, H. Zhu, R. Scinke, Int. J. Bifur. Chaos. **16**, 1913 (2006)
7. C. Jung, H.S. Taylor, E.L. Sibert, J. Phys. Chem. A **110**, 5317 (2006)
8. S. Flach, M.V. Ivanchenko, O.I. Kanakov, Phys. Rev. Lett. **95**, 064102 (2005)
9. J. Ford, Phys. Rep. **213**, 271 (1992); G.P. Berman, F.M. Izrailev, Chaos **15**, 015104 (2005)
10. G. Benettin, L. Galgani, A. Giorgilli, J.-M. Strelcyn, Meccanica **15**, 9 (1980)
11. G. Benettin, L. Galgani, A. Giorgilli, J.-M. Strelcyn, Meccanica **15**, 21 (1980)
12. Ch. Skokos, T.C. Bountis, Ch. Antonopoulos, Physica D **231**, 30 (2007)
13. Ch. Skokos, J. Phys. A **34**, 10029 (2001); Ch. Skokos, Ch. Antonopoulos, T.C. Bountis, M.N. Vrahatis, Prog. Theor. Phys. Supp. **150**, 439 (2003); Ch. Skokos, Ch. Antonopoulos, T.C. Bountis, M.N. Vrahatis, J. Phys. A **37**, 6269 (2004)
14. F.F. Karney, Physica D **8**, 360 (1983); J.D. Meiss, E. Ott, Phys. Rev. Lett. **55**, 2741 (1985); V. Afraimovich, G.M. Zaslavsky, Lect. Notes Phys. **511**, 59 (1998); Ch. Efthymiopoulos, G. Contopoulos, N. Voglis, R. Dvorak, J. Phys. A **30**, 8167 (1997); R. Dvorak, G. Contopoulos, Ch. Efthymiopoulos, N. Voglis, Planet. Space Sci. **46**, 1567 (1998)
15. M. Spivak, *Comprehensive Introduction to Differential Geometry*, Vol. 1 (Publ. or Per. Inc., 1999)
16. Ch. Antonopoulos, T. Bountis, Romai J. **2**, 1 (2006); see also Ch. Antonopoulos, Ph.D. Thesis, Department of Mathematics, University of Patras, 2007
17. J.H. Hubbard, B.B. Hubbard, *Vector Calculus, Linear Algebra and Differential Forms: A Unified Approach*, Chapter 5 (Prentice Hall, 1999)
18. N. Bourbaki, *Éléments de mathématique, Livre II: Algèbre*, Chapitre 3 (Hermann, 1958)
19. W.H. Press, S.A. Teukolsky, W.T. Vetterling, B.P. Flannery, *Numerical Recipes in Fortran 77: The Art of Scientific Computing*, Chapter 2 (Cambridge University Press, 2003)
20. R.I. McLachlan, G.R.W. Quispel, J. Phys. A **39**, 5251 (2006)
21. P.J. Prince, J.R. Dormand, J. Comp. Appl. Math. **7**, 67 (1981)
22. E. Christodoulidi, T. Bountis, Romai J. **2**, 37 (2006)
23. O. Merlo, L. Benet, Cel. Mech. Dyn. Astr. **97**, 49 (2007)